Ammonium Nitrate Cluster Ions

ARTICLE *in* THE JOURNAL OF PHYSICAL CHEMISTRY · MARCH 1996

Impact Factor: 2.78 · DOI: 10.1021/jp9516755

Ammonium Nitrate Cluster Ions

Brett I. Dunlap* and Robert J. Doyle, Jr.

Chemistry Division, Code 6100, Naval Research Laboratory, Washington, D.C. 20375

Received: June 15, 1995; In Final Form: December 15, 1995[⊗]

Sputtering of condensed-phase ammonium nitrate yields many positive and negative cluster ion series derived from different ionic cores. The cluster cores are surrounded by varying numbers of ammonium nitrate monomer units. Most interesting is the extensive series of negative cluster ions of the form $[(NH_4NO_3)_nNO_3]^-$, $n \geq 3$. The corresponding positive clusters, $[(NH_4NO_3)_nNH_4]^+$, are also very extensive but also include the smallest ions, $n = 1$ and 2. Collision-induced dissociation of mass-selected cluster ions suggests that the first two members of the negative series, $n = 1$ and $n = 2$, are not detected because they rearrange and lose one or more ammonia molecules. Gradient-density-functional calculations using two different functionals predict that NH_4NO_3 is strongly hydrogen bonded and that $[(NH_4NO_3)NO_3]^-$ has no hydrogen bonds. This is consistent with this ion rearranging by loss of NH_3 to form the strongly hydrogen-bonded ion $[H(NO_3)_2]^-$. Rearrangements involving loss of ammonia molecules in the negative-ion spectrum and nitric acid molecules in the positive-ion spectrum lead to a rich variety of other, less extensive, series of sputtered ions from this complex solid. Both relative gradient-density-functional energies correlate well with whether or not various ions are observable experimentally.

Introduction

Ammonium nitrate (AN) is a complex solid, having five different stable crystalline phases that exist between slightly below room temperature and its melting point at 169 °C.[1−7] As its name implies, one view of ammonium nitrate (AN) is that of an ionic solid made up of ammonium cations and nitrate anions. If this were the definitive description of the solid, then sputtering might be expected to yield ions of the form $[(NH_4NO_3)_nNH_4]^+$ as the only singly-charged ions in the positive-ion spectrum and ions of the form $[(NH_4NO_3)_nNO_3]^-$ as the only singly-charged ions in the negative-ion spectrum. We will refer to these ionic series as the principal series. The positive-ion principal series, including $n = 1-43$, is indeed observed upon sputtering AN.[8,9] However, the sputtered negative-ion spectrum is not as expected from this simple ionic model. Only the principal-series negative ions, $[(NH_4NO_3)_nNO_3]^-$ $n \geq 3$, occur in significant abundance.[10] The negative cluster ions with $n = 1$ and 2 are observed only in trace amounts. The very low abundance of these ions and the much higher abundance of other positive- and negative-ion series can be rationalized as a consequence of a competing hydrogen-bonded description of AN. All phases of crystalline AN except the high-temperature phase are found to have significant hydrogen-bonded character.[7]

The key to understanding the complexity of the mass spectra of sputtered of AN requires that we consider the effect of hydrogen bonding on the structure of the AN monomer. Transfer of a proton from the ammonium cation to the nitrate anion creates a formula unit that is an ammonia molecule complexing through its lone-pair orbital to nitric acid. The resonance between the ionic and molecular interactions is hydrogen bonding, and we will show that the strength of the hydrogen bond can be correlated with how far a proton is separated from each ammonium cation.

AN is a complicated solid, and the sputtering process itself is complicated. Not only can the sputtering process eject clusters of AN formula units, but one or more of these formula units can be cleaved. Furthermore, any formula unit can be cleaved to either side of the hydrogen bond. If the bond is cleaved to one side, then a positive ammonium ion is separated from a negative nitrate ion. If the hydrogen bond is cleaved to the other side, then a neutral ammonia molecule is separated from a neutral nitric acid molecule. Thus, the cluster ions that might be expected to be observed can be categorized as containing a number of intact formula units, a number of excess ammonia or nitric acid molecules, and a number of excess ammonium cations or nitrate anions. In addition to the principle-series ions defined above, cluster ions containing a single extra ammonia molecule are seen in the positive spectra[8,9] and cluster ions containing one to three extra nitric acid molecules are seen in the negative spectra.[10] We suggest that the extra nitric acid molecules in the negative spectra arise from rearrangement and loss of ammonia from corresponding principal-series ions.

This work examines the structures of the smaller ions and tests whether the relative energetics of the various dissociation pathways correlate with positive and negative ions seen in the spectra. Specifically, we are most interested in the delicate balance between ionic and molecular bonding and how these subtle effects may explain the absence of the $n = 1$ and 2 ions in the sputtered negative-ion mass spectrum and the dominance of the $n = 1$ and 2 ion in the positive-ion mass spectrum.

Experiment

In this work, the AN mass spectra were measured with a ZAB−2F (VG Analytical Ltd.) reverse-geometry, double-focusing mass spectrometer operated with an accelerating potential of 8 kV. Samples were prepared by pressing ammonium nitrate into indium foil affixed to the tip of a fast−atom bombardment probe. Xenon atoms with an average kinetic energy of 6.5 keV were generated using a saddle-field gun operating at 8 kV with an ion current of 1.5 mA. The xenon neutral current equivalent to 7 μA impacted a target area of 4 mm^2.

Figure 1 shows part of the positive-ion mass spectrum of Xe-sputtered ammonium nitrate. The principle-series clusters with

[⊗] Abstract published in *Advance ACS Abstracts,* March 1, 1996.

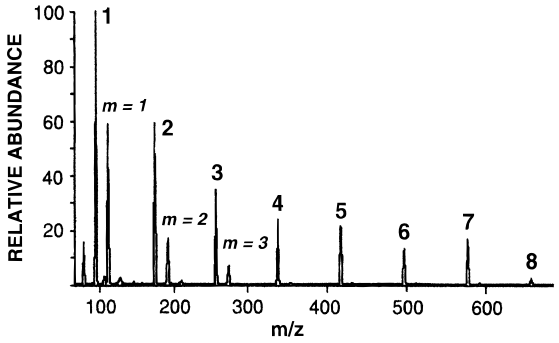

Figure 1. Part of the positive-ion sputtered mass spectrum of ammonium nitrate. The principal-series ions are indicated by numbers. The peaks labeled by $m = 1$, 2, and 3 correspond to the series $[(NH_4NO_3)_mNH_3NH_4]^+$, which is related to the principal-series ion of the next higher number by the loss of a single nitric acid HNO_3 molecule.

the general formula $[(NH_4NO_3)_nNH_4]^+$ are numbered 1−8. The only other abundant ions in the figure are indicated by $m = 1-3$ and are related to the next higher mass principal-series ion by the loss of a nitric acid molecule. The abundance of the principal-series ion falls nearly monotonically with increasing mass in the figure. Figure 2 shows the spectrum of Xe-sputtered ammonium nitrate. The principal-series clusters with the general formula $[(NH_4NO_3)_nNO_3]^-$ are numbered 1−9. Cluster ions with $n = 3-40$ are observed in relatively high abundance; the $n = 1$ ion is almost lost in the noise, and the $n = 2$ ion is far less abundant than the larger members of the series. At lower masses, the abundance of species that are formed by losses of single and multiple NH_3 molecules from principal-series ions becomes pronounced. These are designated a, b, and c, corresponding to losses of 1, 2, and 3 ammonia molecules from principal-series ions. Loss of NH_3 from $[(NH_4NO_3)NO_3]^-$ (the $n = 1$ negative ion) creates $[H(NO_3)_2]^-$, the second most abundant ion (after $[NO_3]^-$) in the spectrum. The specific case that all possible ammonia molecules are lost, for example losing $(NH_3)_3$ from $[(NH_4NO_3)_3NO_3]^-$ ($n = 3$), results in the negative-ion series $[(HNO_3)_mNO_3]^-$, which is designated $m = 1-3$ in Figure 2. These same hydrated nitrate clusters, $m = 1-3$, have been studied by high-pressure mass spectrometry to determine their relative enthalpies of clustering.[11]

To test our hypothesis that the $n = 1$ and 2 negative ions rearrange and fragment, we performed collision-induced-dissociation (CID) experiments on precursor cluster ions. The fairly abundant sputtered negative ions in the spectrum can be mass-selected using the magnetic sector of the mass spectrometer. The mass−selected species are then collided with helium in the field-free region of the instrument; the resultant fragment ions are subsequently detected and identified.[12,13] The $n = 1$ cluster ion is observed in very low abundance from CID of all AN clusters ($n = 3-15$). Figure 3 shows the negative-ion CID spectrum of $[(NH_4NO_3)_7NO_3]^-$. As in Figure 2, the principal-series clusters $[(NH_4NO_3)_nNO_3]^-$, $n = 1-7$, are numbered. Dissociation of these ions forms ions designated a, b, and c, which result from losses of 1, 2, and 3 ammonia molecules, respectively. The relative abundances of ions in the CID spectra are similar to those seen in the directly sputtered mass spectrum. For all parent cluster ions examined, $[(NH_4NO_3)NO_3]^-$ was observed in very low abundance. These results suggest that $[(NH_4NO_3)NO_3]^-$ readily dissociates to form $[H(NO_3)_2]^-$ by loss of NH_3.

Discussion

Both the positive-ion and the negative-ion mass spectra of sputtered ammonium nitrate are more complicated than a simple

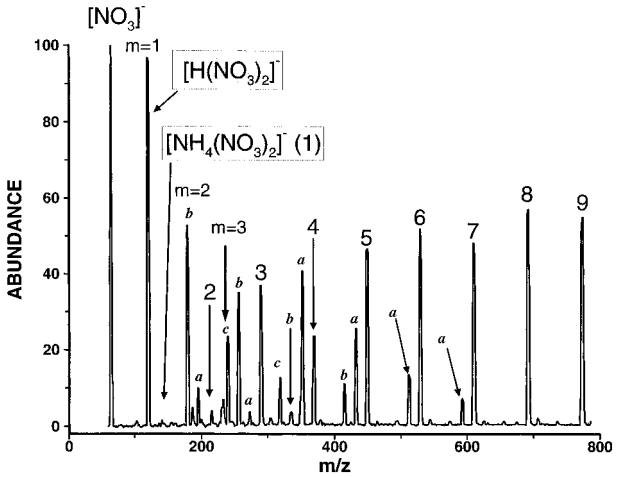

Figure 2. Part of the negative-ion sputtered mass spectrum of ammonium nitrate. The principal-series ions are indicated by numbers. Losses of 1, 2, and 3 ammonia molecules from principal-series ions result in the series labeled by a, b, and c, respectively. Loss of all possible ammonia molecules from the smallest principal-series ions results in the hydrated nitrate series, $m = 1-3$.

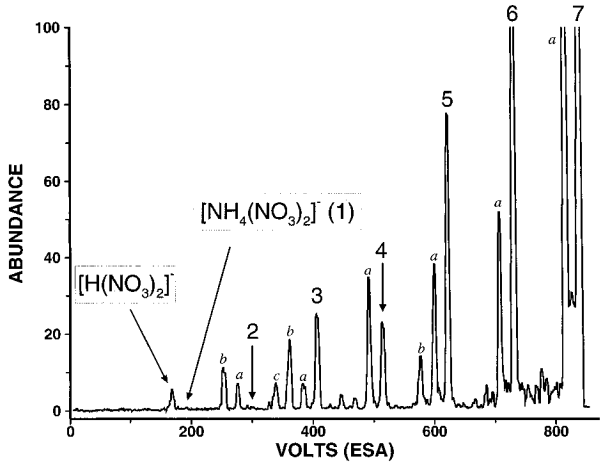

Figure 3. Collision-induced-dissociation (CID) spectrum of $[(NH_4NO_3)_7NO_3]^-$. The ion series are labeled as in Figure 1.

ionic model would predict. Previous work on positively charged ammonium nitrate clusters, under the same experimental conditions, identified the principal cluster-ion series, $[(NH_4NO_3)_nNH_4]^+$, $n = 1$ to >43 inclusive.[9] This series is expected from a simple ionic model. On the other hand, that work also showed that these positive cluster ions can rearrange and dissociate by the loss of a single HNO_3 molecule. In contrast, the principal-series negative-ion clusters dissociate by losses of one to three NH_3 molecules and the $n = 1$ and 2 species from the corresponding negative-ion series are detected in only very low abundance.

These experimental results are insufficient by themselves to answer the question of why there is so little $n = 1$ species in the negative-ion spectra, while the corresponding $n = 1$ species is always abundant in the positive-ion spectra. The lack of thermodynamic data for many of these species mandates a purely theoretical approach for analysis.

Density-functional (DF) theory[14,15] is an appropriate method for studying AN clusters where both ionic and hydrogen bonding interactions contribute to determining structures and energetics. Exchange and correlation functionals of the density gradient, in addition to the density itself, are essential because of the hydrogen bonding and our desire to compare relative total energies.[16−18] The deMon[19,20] computer code was employed, which uses three different Gaussian basis sets:[21] one to fit the

TABLE 1: Optimized Becke Exchange [23] and Perdew [24,25] Correlation Density-Functional Total Molecular Energies in Hartree Atomic Units

molecule	energy	positive ion	energy	negative ion	energy
NH_3	−56.5703	$[NH_4]^+$	−56.9104	$[NO_3]^-$	−280.4672
HNO_3	−280.9928	$[NH_4NH_3]^+$	−113.5294	$[H(NO_3)_2]^-$	−561.5110
NH_4NO_3	−337.5876	$[NH_5NO_3]^+$	−337.9271	$[NH_4(NO_3)_2]^-$	−618.1067
		$[(NH_4)_2NO_3]^+$	−394.5503		

TABLE 2: Perdew Exchange [24,25] and Perdew Correlation [26] Density-Functional Total Molecular Energies in Hartree Atomic Units[a]

molecule	energy	positive ion	energy	negative ion	energy
NH_3	−56.6289	$[NH_4]^+$	−56.9667	$[NO_3]^-$	−280.7229
HNO_3	−281.2475	$[NH_4NH_3]^+$	−113.6458	$[H(NO_3)_2]^-$	−562.0237
NH_4NO_3	−337.9031	$[NH_5NO_3]^+$	−338.2406	$[NH_4(NO_3)_2]^-$	−618.6817
		$[(NH_4)_2NO_3]^+$	−394.9248		

[a] These energies are calculated at the geometries found in obtaining Table 1.

one-electron orbitals, one to fit the exchange-correlation part of the electronic potential, and one to fit the density to obtain the Coulomb part of the electronic potential variationally.[22] The default double-ζ plus polarization-on-heavy-atoms basis set was used with either the Becke[23] or Perdew[24,25] density-gradient exchange potential and the Perdew[26] density-gradient correlation potential. Building on our previous study of the negative ions,[10] we optimized the geometries of additional positive and neutral AN clusters using the Becke exchange functional. The total energies calculated using the Becke exchange for selected small neutrals, cations, and anions are given in Table 1. The Perdew exchange functional gives larger hydrogen-bond energies than does the Becke functional.[17,18] For the case of water, higher hydrogen-bond energies are in better agreement with high-level ab initio results,[27] but overall the Becke exchange functional gave slightly better results for hydrogen-bonded systems than the Perdew exchange functional.[18] The differences in optimized geometries using the two density-gradient exchange functionals are quite small.[17,18] This is consistent with earlier work suggesting that geometries are quite well converged within density-functional theory even at the local-density-approximation level.[15,28] Thus, the electronic energies given in Table 2 for the Perdew exchange at the Becke-exchange-optimized geometries are likely very close to the values that would be obtained upon full optimization. Relative energies, the focus of this work, should be quite accurate for both exchange functionals.

Optimizing the equilibrium structures of these molecules and ions is a good way to gain insight into the energetics. Figure 4 depicts the optimized structure of ammonium nitrate, NH_4NO_3. The atoms, from darkest to lightest, are nitrogen, oxygen, and hydrogen. The fourth hydrogen atom of the NH_4 group is pulled away by 0.6 Å toward the NO_3 group. This structure agrees very well with that computed at the Hartree−Fock (HF) level of theory using a 4-31G Gaussian basis set.[29] The ammonia nitrogen to nitrate hydrogen distance is 1.63 Å compared to the HF result of 1.617 Å. The average difference between the two types of NO bonds in the nitrate ion is 0.16 Å compared to the HF difference of 0.177 Å. The HON angle is 105° compared to the HF angle of 110.0°. Viewed as a molecule formed from ammonia and nitric acid components, the Becke−Perdew (BP) and Perdew−Perdew (PP) DF bonding energies of AN are 15.4 and 16.8 kcal/mol, respectively. This binding energy is somewhat less than 21.7 kcal/mol obtained in the HF calculation. Nevertheless, these DF calculations also support the conclusion that AN contains one of the strongest known hydrogen bonds.[29] Viewed as formed from an ammonium cation and a nitrate anion, its binding energy would be 132 (BP) or 134 kcal/mol (PP).

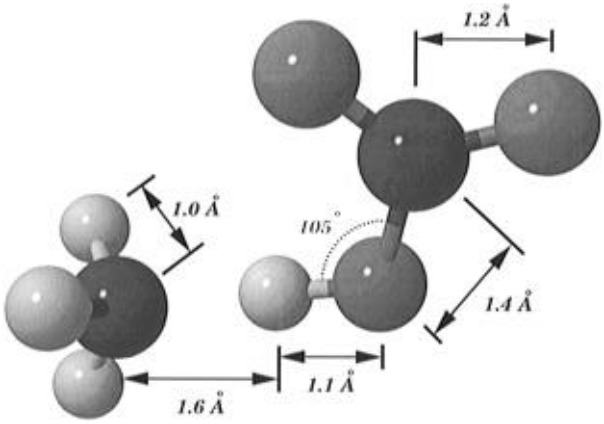

Figure 4. Ball-and-stick images of NH_4NO_3. The geometry was obtained by optimizing the Becke−Perdew (BP) density-functional (DF) energy. From lightest to darkest, the atoms are hydrogen, oxygen, and nitrogen. Note that one of the hydrogen atoms is clearly associated with the NO_3 group.

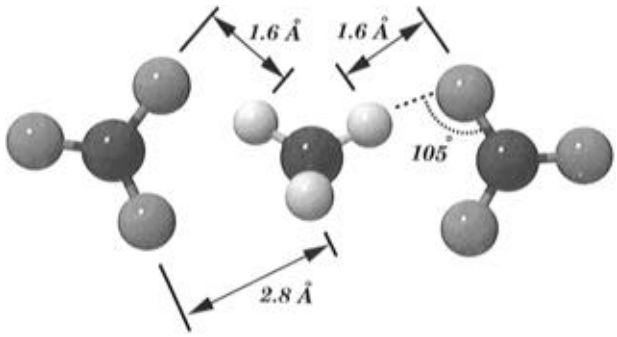

Figure 5. Optimized geometry of $[NH_4(NO_3)_2]^-$. Note that all hydrogen atoms are clearly associated with the ammonium nitrogen atom.

Figure 5 shows the optimized structure of $[NH_4(NO_3)_2]^-$. The 1.6 Å minimum distance between oxygen and hydrogen atoms indicates essentially no hydrogen bonding in this ion.[10] The in-plane NH bonds average 1.08 Å, and the out-of-plane NH bonds average 1.03 Å. Viewed as formed from AN and $[NO_3]^-$, its DF binding energy is 32.6 kcal/mol (BP) or 35.0 kcal/mol (PP).

Figure 6 shows the optimized structue $[(NH_4)_2NO_3]^+$. The 1.5 Å distance between the oxygen and hydrogen atoms is a consequence of two weak hydrogen bonds. These bonds are slightly stronger than those in the corresponding negative ion of Figure 5. The N−H bond distances to H atoms closest to the nitrate group are quite long, 1.13 Å. The other N−H bonds are all 1.03 Å. There is a slight difference in NO bond distances. The NO distances to the oxygen atoms nearest hydrogen atoms

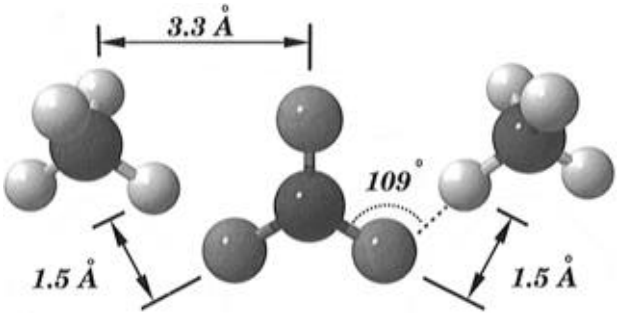

Figure 6. Optimized geometry of $[(NH_4)_2NO_3]^+$. Note that the NH bonds pointing toward oxygen atoms are elongated but still clearly associated with ammonium nitrogen atoms.

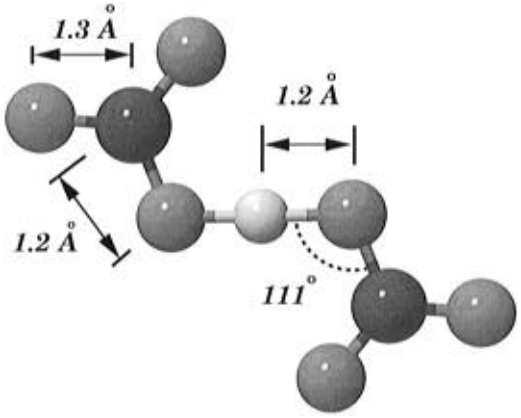

Figure 7. Optimized C_{2h} structure of $[H(NO_3)_2]^-$.

in the ammonium ions average 1.28 Å in contrast to the third NO bond distance of 1.26 Å. Viewed as formed from AN and $[NH_4]^+$, the $[(NH_4)_2NO_3]^+$ DF binding energy is 32.8 (BP) or 34.5 kcal/mol (PP). The binding energies of the positive and negative $n = 1$ principal-series ions are essentially the same in this purely ionic description of the bonding.

Alternatively, the $n = 1$ ions from both the positive and negative spectra could yield other species upon neutral cleavage of their AN monomer unit. In principle, $[(NH_4NO_3)NO_3]^-$ could lose HNO_3, to yield $[NH_3NO_3]^-$. This ion has not been seen in any of our experimental work. Loss of the other neutral fragment, NH_3, yields $[H(NO_3)_2]^-$, which is depicted in Figure 7 in its optimized C_{2h} structure. This is the structure of hydrogen dinitrate seen in tetraphenylarsonium.[30] In this strongly hydrogen-bonded ion, the O−H bond distances are 1.2 Å, in agreement with an analysis of X-ray diffraction data.[31]

$[H(NO_3)_2]^-$ rotates readily around the O−H−O bond. Rotating by 180° around this bond yields a C_{2v} structure that lies 1.9 kcal/mol higher in BP DF energy. Rotation by 157° is seen experimentally in cesium hydrogen dinitrate,[32] and rotation by roughly 90° is seen in $Rh(C_5H_5N)_4H(NO_3)_2$.[33] The 90° structure is lower in energy than the 0° structure by 37 kcal/mol in a minimum-basis-set HF calculation.[34] The nonplanar structure is also the lowest-energy structure, by 1.6 kcal/mol (BP), in our DF calculations. The energies for the nonplanar structure are included in Tables 1 and 2. In the optimized nonplanar configuration, the NO_3 units are flat but twisted to give varying dihedral angles. The N−O−O−N dihedral angle is 99°. The O−O−O−O dihedral angles connecting the other two pairs of C_2-symmetry-equivalent atoms through the hydrogen-bonded oxygen atoms are 94° and 108°. Viewed as formed from nitric acid and $[NO_3]^-$, the density-functional binding energy of $[H(NO_3)_2]^-$ is quite large, 32.0 (BP) or 33.5 kcal/mol (PP). Consequently, viewed as formed from this ion and ammonia, the binding of the $n = 1$ negative ion is quite small, 15.9 (BP) or 18.3 kcal/mol (PP).

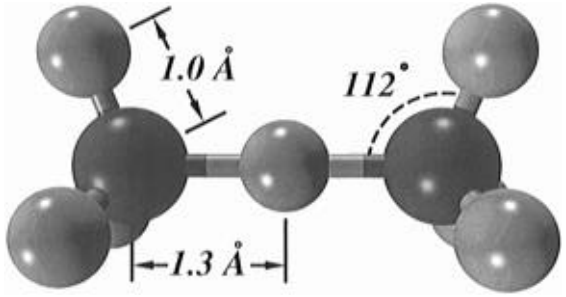

Figure 8. Optimized structure of $[NH_4NH_3]^+$.

Looking again at the positive ions, $[NH_4NH_3]^+$ and $[HNO_3NH_4]^+$, which correspond to losses of both neutral AN fragments from the $n = 1$ positive ion, are observed experimentally in the positive-ion mass spectrum.[9] Loss of HNO_3 from $[(NH_4NO_3)NH_4]^+$ yields $[NH_4NH_3]^+$, which is depicted in Figure 8. This is another strongly hydrogen-bonded ion. Viewed as formed from ammonia and $[NH_4]^+$, its binding energy is 30.6 (BP) or 31.5 kcal/mol (PP). Loss of the other neutral fragment, ammonia, yields $[HNO_3NH_4]^+$. There is very little hydrogen bonding in this ion; the second shortest OH bond is 1.7 Å. Viewed as formed from $[NH_4]^+$ and ammonia, this ion's bonding energy is only 15.0 (BP) or 16.7 kcal/mol (PP). Thus the positive $n = 1$ ion has a greater tendency to lose nitric acid than ammonia. Viewed as formed from nitric acid and $[NH_4NH_3]^+$, the binding energy of $[(NH_4NO_3)NH_4]^+$ is 17.6 (BP) or 19.8 kcal/mol (PP). Viewed as formed from ammonia and $[HNO_3NH_4]^+$, its binding energy is 33.2 (BP) or 34.7 kcal/mol (PP). Experimentally, ammonia loss slightly dominates nitric acid loss from the collisionally-activated $n = 1$ principal-series ion. However, nitric acid loss dominates ammonia loss from the collisionally-activated $n > 1$ principal-series positive ions.[9] With regard to either neutral-cleavage decay channel and using either DF, these binding energies are both larger than the binding energies of the corresponding $n = 1$ principal-series negative ion. Ammonia loss requires considerably less energy than AN loss from the $n = 1$ negative ion, and nitric acid loss requires considerably less energy than AN loss from the $n = 1$ positive ion. These significant energy differences are responsible for the different dissociation pathways observed in these ions.

Conclusions

With regard to the lowest-energy dissociation pathways, DF calculations show that $[(NH_4NO_3)NH_4]^+$ has greater binding energy than $[(NH_4NO_3)NO_3]^-$. The calculations show that the hydrogen bonding in the positive ion is greater than in the negative ion. This is consistent with the fact that the positive ion is seen in the sputtered spectrum and that the negative ion is not seen in significant abundance. These calculations predict that if the negative ion were created with less than 15.9 (BP) or 18.3 kcal/mol (PP) of internal energy, then it would be stable to dissociation. The calculations are consistent with the experimental observation that the principal negative-ion series, $[(NH_4NO_3)_nNO_3]^-$, is related to the other abundant negative ion series by loss of one or more ammonia molecules, while the principal positive-ion series, $[(NH_4NO_3)_nNH_4]^+$, is related to the other abundant positive-ion series by loss of one nitric acid molecule.

Consistent with other work using gradient-density-functionals,[17,18] the hydrogen-bond energies predicted by the Perdew exchange are consistently slightly larger than those predicted

by the Becke exchange. Using either Becke exchange or Perdew exchange, the dissociation energy of the $n = 1$ negative ion is approximately 2 kcal/mol less than that of the positive ion.

Nitric acid is known to be much more weakly bound to positive ions (also acids) than ammonia. Loss of nitric acid is seen in the positive spectrum (Figure 1). Ammonia (a base) is known to be much more weakly bound to negative ions (also bases) than nitric acid.[34−36] Loss of ammonia is seen in the negative spectra of Figures 2 and 3. Our experimental and theoretical data agree to suggest that the former effect is smaller than the latter effect for the case of small ammonium nitrate cluster ions. That we do not experimentally see such a difference in our spectra for the larger ions might be due to the dispersal of the excess charge over a larger volume or to the fact that an ionic model, which does not energetically distinguish positive and negative principal-series ions, becomes more valid with increasing mass.

Acknowledgment. B.I.D. thanks Dennis Salahub for inclusion in the deMon collaboration. R.J.D. expresses his gratitude to D.A.D. This work was supported by the Propulsion and Energetic Materials Program of the Mechanics Division of the Office of Naval Research, the Physics Division (Contact #N00014-95-WX-20010) of the Office of Naval Research, and the Naval Research Laboratory Energetic Materials Accelerated Research Initiative.

References and Notes

(1) Shinnaka, Y. *J. Phys. Soc. Jpn.* **1959**, *14*, 1073−1083.
(2) Amorós, J. L.; Arrese, F.; Canut, M. *Z. Kristallogr.* **1962**, *117*, 92−107.
(3) Choi, C. S.; Mapes, J. E.; Prince, E. *Acta Crystallogr.* **1972**, *B*28, 1357−1361.
(4) Ahtee, M.; Kurki-Suonio, K.; Lucas, B. W.; Hewat, A. W. *Acta Crystallogr.* **1979**, *A35*, 591−597.
(5) Lucas, B. W.; Ahtee, M.; Hewat, A. W. *Acta Crystallogr.* **1979**, *B*35, 1038−1041.
(6) Choi, C. S.; Prask, H. J.; Prince, E. *J. Appl. Crystallogr.* **1980**, *13*, 403−409.
(7) Choi, C. S.; Prask, H. J. *Acta Crystallogr.* **1982**, *B38*, 2324−2338.
(8) Doyle, R. J., Jr. *J. Am. Chem. Soc.* **1993**, *115*, 5300−5301.
(9) Doyle, R. J., Jr. *J. Am. Chem. Soc.* **1994**, *116*, 3005−3011.
(10) Doyle, R. J., Jr.; Dunlap, B. I. *J. Phys. Chem.* **1994**, *98*, 8261−8263.
(11) Lee, N.; Keesee, R. G.; Castleman, A. W., Jr. *J. Chem. Phys.* **1980**, *72*, 1089−1094.
(12) Doyle, R. J., Jr. *J. Am. Chem. Soc.* **1988**, *110*, 4120−4126.
(13) Doyle, R. J., Jr. *J. Org. Mass Spectrom.* **1993**, *28*, 83−91.
(14) Parr, R. G.; Yang, W. *Density Functional Theory of Atoms and Molecules*; Oxford University Press: Oxford, 1989.
(15) Ziegler, T. *Chem. Rev.* **1991**, *91*, 651−667.
(16) Andzelm, J.; Wimmer, E. *J. Chem. Phys.* **1992**, *96*, 1280−1303.
(17) Sim, F.; St.-Amant, A.; Papai, I.; Salahub, D. R. *J. Am. Chem. Soc.* **1992**, *114*, 4391−4400.
(18) Mijoule, C.; Latajka, Z.; Borgis, D. *Chem. Phys. Lett.* **1993**, *208*, 364−368.
(19) Salahub, D. R.; Fournier, R.; Młynarski, P.; Papai, I.; St.-Amant, A.; Ushio, J. In *Density Functional Methods in Chemistry*; Labanowski, J., Andzelm, J., Eds.; Springer: New York, 1991; pp 77−100.
(20) St.-Amant, A.; Salahub, D. R. *Chem. Phys. Lett.* **1990**, *169*, 387−392.
(21) Sambe, H.; Felton, R. H. *J. Chem. Phys.* **1975**, *62*, 1122−1126; **1974**, *61*, 3862−3863.
(22) Dunlap, B. I.; Connolly, J. W. D.; Sabin, J. R. *J. Chem. Phys.* **1979**, *71*, 3396−3402, 4993−4999.
(23) Becke, A. D. *Phys. Rev. A* **1988**, *38*, 3098−3100.
(24) Perdew, J. P. *Phys. Rev. Lett.* **1985**, *55*, 1665−1668.
(25) Perdew, J. P.; Wang, Y. *Phys. Rev. B* **1986**, *33*, 8800−8802; **1989**, *40*, 3399(E).
(26) Perdew, J. P. *Phys. Rev. B* **1986**, *33*, 8822−8824.
(27) Szalewicz, K.; Cole, S. J.; Kołos, W.; Bartlett, R. J. *J. Chem. Phys.* **1988**, *89*, 3662−3673.
(28) Fan, L.; Ziegler, T. *J. Chem. Phys.* **1991**, *94*, 6057−6063; *J. Phys. Chem.* **1992**, *96*, 6937−6941.
(29) Latajka, Z.; Szczęśniak, M. M.; Ratajczak, H.; Orville-Thomas, W. J. *J. Comput. Chem.* **1980**, *1*, 417−419.
(30) Faithful, B. D.; Wallwork, S. C. *Chem. Commun.* **1967**, 1211.
(31) Barlič, B.; Hadži, D.; Orel, B. *Spectrochim. Acta* **1981**, *37A*, 1047−1048.
(32) Rozière, J.; Rosiere-Bories, J.-T.; Williams, J. M. *Inorg. Chem.* **1976**, *15*, 2490−2494.
(33) Rozière, J.; Lehmann, M. S.; Potier, J. *Acta Crystallogr.* **1979**, *35*, 1099−1102.
(34) Gunde, R.; Šolmajer, T.; Ažman, A.; Hadži, D. *J. Mol. Struct.* **1975**, *24*, 405−408.
(35) Larson, J. W.; McMahon, T. B. *J. Am. Chem. Soc.* **1984**, *106*, 517−521.
(36) Evans, D. H.; Keesee, R. G.; Castleman, A. W., Jr. *J. Chem. Phys.* **1987**, *86*, 2927−2931.
(37) Keesee, R. G.; Castleman, A. W., Jr. *J. Phys. Chem. Ref. Data* **1986**, *15*, 1011−1071.

JP9516755